Polymer overlayers tune electromagnetically induced transparency in a two-dimensional semiconductor

Kai-Qiang Lin, Robert Martin, Sebastian Bange, John M. Lupton*

Institut für Experimentelle und Angewandte Physik, Universität Regensburg, Universitätsstraße 31, 93053 Regensburg, Germany

ABSTRACT: Electromagnetically induced transparency (EIT) arises because of quantum interference between different electronic transitions of a material. While the phenomenon is considered a gold standard in atomic quantum optics, it is exceedingly hard to probe in the condensed phase – a prerequisite for exploiting the effect in devices. EIT arises naturally in strong excitonic transitions of single-layer transition-metal dichalcogenide crystals, which in effect constitute giant two-dimensional exfoliated molecules. We exploit the characteristic sensitivity of molecules to their immediate dielectric environment to demonstrate how chemical tuning of the exciton resonance over almost 5 % of the exciton transition energy allows unprecedented control over the quantum-interference phenomenon. EIT is probed in the surface second-harmonic generation (SHG) of monolayer WSe_2, where it gives rise to resonant suppression of SHG in direct response to the immediate surrounding. This solid-state solvatochromic effect arises primarily from changes in the electronic bandgap and exciton binding energy of monolayer WSe_2. Surprisingly, we find that the EIT resonance shifts linearly with the fundamental exciton resonance. The approach demonstrates that concepts from atomic quantum optics can be ported directly to materials in the condensed phase, stimulating new synthetic challenges to develop materials to tune coherent phenomena.

When a classical harmonic oscillator is driven too hard on resonance, bonds break because displacement from equilibrium becomes too large. The description of oscillations in a quantum-mechanical system is not fundamentally different from the classical picture, although it is typically formulated in the framework of the population density of each quantum state. Because the oscillation is expressed in terms of oscillating population densities of states, resonant driving of the oscillation can be described as a driven transition between states – stimulated absorption and emission. This simple concept lies at the heart of magnetic resonance spectroscopy and atomic and molecular quantum optics, and is trivially visualized with a two-level system. Driving the system on resonance with an oscillating electromagnetic field leads to population transfer from the ground state $|1\rangle$ to the excited state $|2\rangle$. However, if the two-level system is already in the excited state, the electromagnetic field induces stimulated emission from $|2\rangle \rightarrow |1\rangle$. In this perturbative semi-classical reasoning, stimulated emission will compete with stimulated absorption so that the time and ensemble averaged population density of the excited state $|2\rangle$ does not exceed 50 %. A non-perturbative quantum-mechanical treatment of the problem reveals a richer interaction between the two-level system and the electromagnetic field. Since the driving field induces both $|1\rangle \rightarrow |2\rangle$ and $|2\rangle \rightarrow |1\rangle$ transitions, coherent Rabi oscillations in population density arise, the frequency of which depend solely on the driving-field amplitude and the degree of detuning of the driving field from the two-level system resonance. Such Rabi oscillations report on the quantum-mechanical coherence of the two-level system, i.e. the duration over which a state retains information on the phase of its wavefunction. Rabi oscillations are familiar from their role in magnetic resonance imaging and spectroscopy, and are central to all concepts of quantum-information processing and quantum computing. However, in contrast to magnetic-dipole transitions of spins and electric-dipole transitions in atoms, it can be challenging to drive transitions in materials in the condensed phase sufficiently strongly to exhibit quantum-mechanical coherence effects: they disintegrate when driven too hard.

Most real-world objects do not fit the simple picture of a two-level system. Adding only one additional level opens up a host of new phenomena. Figure 1a sketches the possible optical transitions in a three-level system. Here, because of the dipole-selection rules, the $|1\rangle \rightarrow |2\rangle$ and $|2\rangle \rightarrow |3\rangle$ transitions are allowed, but the $|3\rangle \rightarrow |1\rangle$ transition is forbidden. Quantum interference occurs between the two allowed transition pathways: it is trivial that pumping $|1\rangle \rightarrow |2\rangle$ opens up the $|2\rangle \rightarrow |3\rangle$ transition, but for strong drive, coherent Rabi flopping will occur between $|2\rangle \leftrightarrow |3\rangle$ so that the $|3\rangle \rightarrow |2\rangle$ transition interferes destructively with the $|1\rangle \rightarrow |2\rangle$ transition. Because of this interference, an electromagnetically induced transparency (EIT) emerges on the first ground-state transition ($|1\rangle \rightarrow |2\rangle$). Typically, EIT is probed in atomic gases using non-degenerate control ($|2\rangle \rightarrow |3\rangle$) and probe ($|1\rangle \rightarrow |2\rangle$) transitions.[1]

Only very few examples of EIT exist in the condensed phase.[2] EIT is particularly interesting when the two transitions are degenerate and can be driven by one and the same field. In this case, rather than detecting the change in transmission directly, it is appealing to monitor suppressed absorption by a change in the non-linear optical response.[3] Figure 1b indicates the simplest non-linear response to optical driving: a two-photon transition to a virtual state (dashed) which gives rise to frequency doubling in the form of second-harmonic generation (SHG). In an isotropic medium, the solution to Maxwell's equations under a quadratic response of the electric displacement field to an external electric field does not give rise to a propagating wave since electromagnetic waves of opposite amplitude and propagation direction cancel out. SHG only occurs when inversion symmetry is broken. SHG is readily detectable in polar molecules and is a standard technique to study, for example, lipid membranes.[4] SHG can also be pronounced in atomically thin two-dimensional crystal monolayers of exfoliated transition-metal dichalcogenides (TMDCs)[5] – covalently bound objects, which, in effect, are viewed as giant two-dimensional molecules.[6] These semiconductors constitute an intermediate between atoms, molecules and solids in that, just like atoms, they support discrete optical transitions with well-resolved

Rydberg series of the energies of the elementary electron-hole bound state, the exciton.[7] At the same time – and unlike atomic transitions – excitons can move in space, thereby gaining oscillator strength as more electrons interact through one common pathway. This high oscillator strength implies that phenomena associated with strong light-matter coupling[8] can, in principle, be probed without the need of an external cavity.

The crucial appeal of exploring non-linear quantum optics in monolayer crystals is that – since there is no volume to the two-dimensional object – they have in common with molecules the characteristic of maximal surface, making the underlying electronic transitions highly susceptible to changes in the immediate dielectric or chemical environment. Two-dimensional semiconductors show a very strong response to both liquids and solids deposited on them[9] since the field lines of the electrostatically bound exciton respond to changes in the local refractive index Δn, in analogy to the plasmon resonance of noble-metal nanoparticles.[10] This form of "solid-state solvatochromism"[11] offers a unique route to tuning the electronic structure of the system as sketched in Fig. 1b. We use the term here simply to designate the response of the exciton resonance to the immediate molecular environment, noting that this could arise from a host of effects besides the change Δn in dielectric constant: both the polarity of the overlayer material will have an effect as well as strain[12] induced by different thermal coefficients of the materials. In any case, chemical engineering of the environment shifts the exciton resonance and therefore opens up an unprecedented route to controlling the quantum-interference phenomenon EIT illustrated in Figure 1a – something which is not possible in conventional atomic quantum optics. We demonstrate here that the excitonic transitions can be shifted by more than 70 meV, allowing concomitant tuning of the wavelength at which EIT occurs. Such control over fundamental quantum-mechanical effects in light-matter interaction is crucial to developing novel devices based on EIT such as lasers which do not require population inversion,[13] storage units for light,[14] and gates for entangling and processing quantum information.[15]

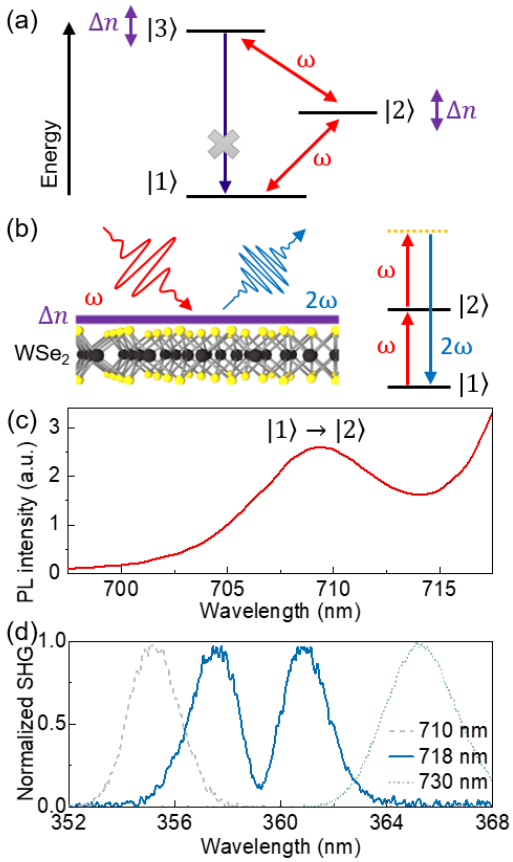

Figure 1. Chemical tuning of electromagnetically induced transparency (EIT) in the surface second-harmonic generation (SHG) of monolayer WSe_2 crystals. (a) Energy-level scheme of the three-level system. Transitions between $|1\rangle$ and $|2\rangle$ and between $|2\rangle$ and $|3\rangle$ are allowed, but not between $|1\rangle$ and $|3\rangle$. If $|2\rangle$ is placed around halfway between $|1\rangle$ and $|3\rangle$, quantum interference will occur between the two allowed transitions. (b) The interference can be probed by resonant SHG, arising from a transition to a virtual state (dashed). SHG is suppressed by EIT arising from the quantum interference. Since the three-level system exists in the condensed phase, the energies of excitonic transitions can be shifted by changing the immediate environment of the WSe_2 monolayer. The shift in resonance with refractive index change Δn constitutes a form of solid-state solvatochromism. (c) Photoluminescence (PL) spectrum of a WSe_2 monolayer on a Si/SiO_2 wafer. The lowest-energy PL peak corresponds to the $|2\rangle \rightarrow |1\rangle$ transition. (d) Corresponding SHG spectra of the sample irradiated by laser pulses of 80 fs duration, close to the exciton resonance, at 710 nm, 718 nm and 730 nm. Under excitation at 718 nm, a minimum in SHG intensity is observed at precisely half the excitation wavelength due to the suppression of SHG by EIT.

Figure 1c shows the photoluminescence (PL) spectrum of the fundamental optical transition of monolayer WSe_2, cleaved from a bulk crystal by an exfoliation process and deposited by a stamp transfer technique[16] on a Si/SiO_2 wafer. The crystal has an overall thickness of 7 Å and lateral extensions of order 100 μm as shown in the microscope image in Fig. S1 of the Supporting Information, is mounted in a cryostat under vacuum at a temperature of 5 K, and is excited with a laser at 488 nm.[3] A clear peak is resolved at 709 nm which corresponds to the lowest-energy excitonic transition of monolayer WSe_2, referred to here as the $|2\rangle \rightarrow |1\rangle$ transition.[3] Panel d plots the resonantly enhanced SHG of the sample irradiated with 80 fs long pulses of a Ti:sapphire laser at 80 MHz repetition rate, pumped at 710 nm, 718 nm, and 730 nm, i.e. in the

vicinity of the exciton resonance. As reported recently,[3] the EIT effect arises naturally in such two-dimensional semiconductors, suppressing absorption close to the exciton resonance and therefore giving rise to a strong reduction of the SHG intensity at half the drive wavelength, when pumped at a wavelength (718 nm) corresponding to half the energy of the $|3\rangle \rightarrow |1\rangle$ transition. Since this transition is dipole-forbidden, it is challenging to probe the nature of state $|3\rangle$ directly. However, as the $|1\rangle \rightarrow |2\rangle$ transition corresponds to the exciton formed between a hole in the highest valence band and an electron in the lowest conduction band of the semiconductor, it is reasonable to conclude that the dark $|3\rangle \rightarrow |1\rangle$ transition arises from a higher-lying conduction band. Such bands are hard to probe experimentally, but recent density-functional theory calculations indicate the presence of a suitable band corresponding to the observed transition energy of the dark exciton required to enable EIT, making the $|1\rangle \rightarrow |2\rangle$ and $|2\rangle \rightarrow |3\rangle$ transitions close to degenerate. [3,17]

We explore the ability to tune the exciton resonance by changing the medium in immediate proximity to the WSe_2 monolayer. As illustrated in Figure 2a-b, we compare samples with bare WSe_2 transferred directly onto the silicon wafer with those in contact with additional layers of exfoliated hexagonal boron nitride (hBN),[18] spin-coated poly(methyl methacrylate) (PMMA), polystyrene (PS), PMMA:PS copolymers, poly(acrylic acid) (PAA), polyethylene (PE) or the transparent polymer Zeonex®. Detailed information on the preparation of these encapsulated samples is given in Ref. [3], and the remaining samples are described in the Supporting Information. We compare different samples and different microscopic spots on each sample since the dielectric constant of the environment can vary over small length scales. Figure 2c-d and Fig. S2 show representative PL spectra of the lowest-energy exciton transition, known as the "A-exciton"[19], of the different samples. The peak positions scatter over 30 nm, corresponding to an energy range of 75 meV, and fall into two larger groups showing bathochromic (panel c) and hypsochromic (panel d) shifts. The lowest-energy transition is found for the double-sided hBN encapsulation, the highest-energy transitions for polymer coverage.

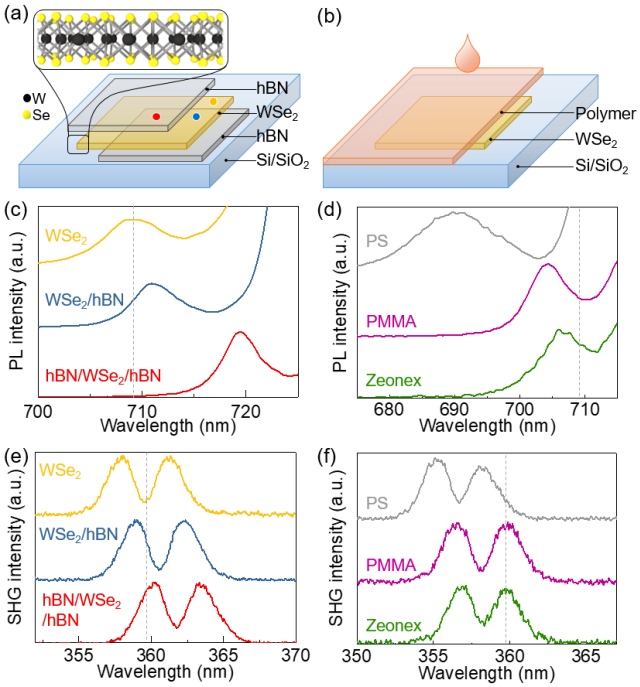

Figure 2. Examples of tuning the excitonic resonance and the EIT phenomenon by either encapsulating monolayer WSe_2 with hBN (a) or by depositing different polymer overlayers on top (b). Plots of PL (c, d) and SHG (e, f) spectra show shifts correlated with changes in dielectric environment. All SHG spectra were recorded after tuning the excitation wavelength to maximize the EIT dip.[3] Grey dashed lines mark the exciton PL peak and the EIT dip position of bare monolayer WSe_2.

The shift in the exciton resonance directly affects the quantum-interference effect. Figure 2e-f plots the corresponding SHG spectra, ordered by the wavelength of the EIT dip. The wavelength of the pump laser was tuned so that the SHG spectrum appears symmetrical and the magnitude of the EIT dip becomes maximal.[3] The EIT feature in SHG can be tuned over a range of 50 meV, from 357 nm to 362 nm. Even though subtle changes in the exciton linewidth appear in the PL in Figure 2c-d, the width of the EIT remains approximately constant. Given the assignment of state $|3\rangle$ to an exciton involving a higher-lying conduction band,[3] we would not expect a fundamental difference in the shift of the exciton energies corresponding to states $|2\rangle$ and $|3\rangle$ with a change in refractive index Δn. Indeed, as plotted in Figure 3, the EIT dip in the SHG spectrum shifts by the same amount as the maximum of the PL peak with a high correlation coefficient of $r = 0.96$. The data points for PS and PE fall outside the correlation. Interestingly, these are the two least polar materials. As shown in Fig. S2, the PL spectrum for these samples is broadened compared to that of bare WSe_2, by a factor of 2.7 in the case of PS. This broadening may be a signature of increased disorder, induced, for example, by strain[12]. Inhomogeneous broadening of the exciton resonance would mask any correlation between PL and EIT resonances.

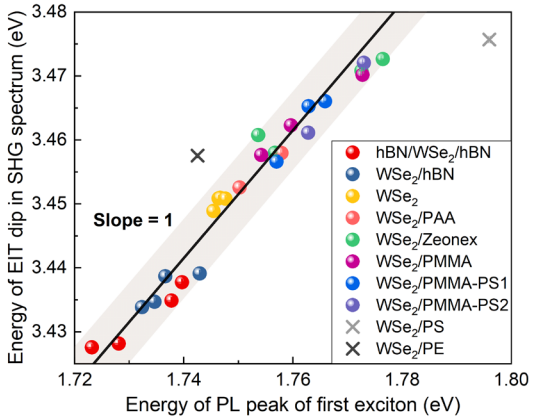

Figure 3. Correlation between the excitonic transition energy and the energy of the EIT dip in SHG for different overlayers (red: hBN/WSe_2/hBN; blue: WSe_2/hBN; yellow: bare WSe_2; green: WSe_2/Zeonex; magenta: WSe_2/PMMA; grey: WSe_2/polystyrene). All samples were deposited on a Si/SiO_2 wafer. The complete data set is shown in Fig. S2.

Elementary atomic quantum optics describes a wide range of often counterintuitive phenomena, which are mostly inaccessible with materials in the condensed phase. The demonstration of EIT in SHG from molecule-like monolayers of WSe_2 shows that concepts of atomic quantum optics can be easily ported to chemically relevant systems: EIT can then be tuned by solid-state solvatochromism, an approach which is not conceivable in conventional atomic-gas systems. Given the extraordinary sensitivity of surface-based nonlinear-optical analytical techniques, we anticipate that exploitation of elaborate quantum-optical concepts such as EIT will allow the design of even more sophisticated spectroscopic methods. In particular, because the excitonic transitions in two-dimensional semiconductors are momentum-space valley selec-

tive[20] – that is, they depend on the handedness of the driving light field – the interaction with the environment should relate to molecular chirality and may open a route to circular dichroism spectroscopy on the nanoscale. The challenge now is to evolve existing methods of molecular self-assembly in the context of two-dimensional materials to arrive at new functionalities exploiting electronic quantum coherence – such as those based on inversionless lasing[13] – which are not conceivable in conventional gas-phase systems.

ASSOCIATED CONTENT

Supporting Information

Information on sample preparation and measurement techniques along with all raw data used to compile Fig. 3. This material is available free of charge via the Internet at http://pubs.acs.org.

Corresponding Author

john.lupton@ur.de

Notes

The authors declare no competing financial interests.

ACKNOWLEDGMENT

Financial support is gratefully acknowledged from the German Science Foundation through SFB 1277 project B3.

REFERENCES

(1) (a) Harris, S. E. Electromagnetically induced transparency. *Phys. Today* **1997,** *50* (7), 36-42. (b) Fleischhauer, M.; Imamoglu, A.; Marangos, J. P. Electromagnetically induced transparency: Optics in coherent media. *Rev. Mod. Phys.* **2005,** *77* (2), 633-673. (c) Harris, S. E. Lasers without inversion – interference of lifetime-broadened resonances. *Phys. Rev. Lett.* **1989,** *62* (9), 1033-1036.

(2) (a) Ham, B. S.; Hemmer, P. R.; Shahriar, M. S. Efficient electromagnetically induced transparency in a rare-earth doped crystal. *Opt. Commun.* **1997,** *144* (4-6), 227-230. (b) Abdumalikov, A. A.; Astafiev, O.; Zagoskin, A. M.; Pashkin, Y. A.; Nakamura, Y.; Tsai, J. S. Electromagnetically Induced Transparency on a Single Artificial Atom. *Phys. Rev. Lett.* **2010,** *104* (19), 193601. (c) Faist, J.; Capasso, F.; Sirtori, C.; West, K. W.; Pfeiffer, L. N. Controlling the sign of quantum interference by tunnelling from quantum wells. *Nature* **1997,** *390* (6660), 589-591. (d) Frogley, M. D.; Dynes, J. F.; Beck, M.; Faist, J.; Phillips, C. C. Gain without inversion in semiconductor nanostructures. *Nat. Mater.* **2006,** *5* (3), 175-178.

(3) Lin, K.-Q.; Bange, S.; Lupton, J. M. Quantum interference in second-harmonic generation from monolayer WSe2. *Nat. Phys.* **2019**, *15*, 242-246.

(4) (a) Stokes, G. Y.; Conboy, J. C. Measuring Selective Estrogen Receptor Modulator (SERM)-Membrane Interactions with Second Harmonic Generation. *J. Am. Chem. Soc.* **2014,** *136* (4), 1409-1417. (b) Tran, R. J.; Sly, K. L.; Conboy, J. C. Applications of Surface Second Harmonic Generation in Biological Sensing. *Annu. Rev. Anal. Chem.* **2017***, 10*, 387-414.

(5) (a) Kumar, N.; Najmaei, S.; Cui, Q. N.; Ceballos, F.; Ajayan, P. M.; Lou, J.; Zhao, H. Second harmonic microscopy of monolayer MoS2. *Phys. Rev. B* **2013,** *87* (16), 161403. (b) Yin, X. B.; Ye, Z. L.; Chenet, D. A.; Ye, Y.; O'Brien, K.; Hone, J. C.; Zhang, X. Edge Nonlinear Optics on a MoS2 Atomic Monolayer. *Science* **2014,** *344* (6183), 488-490. (c) Ribeiro-Soares, J.; Janisch, C.; Liu, Z.; Elias, A. L.; Dresselhaus, M. S.; Terrones, M.; Cancado, L. G.; Jorio, A. Second Harmonic Generation in WSe2. *2D Mater.* **2015,** *2* (4), 045015. (d) Wang, G.; Marie, X.; Gerber, I.; Amand, T.; Lagarde, D.; Bouet, L.; Vidal, M.; Balocchi, A.; Urbaszek, B. Giant Enhancement of the Optical Second-Harmonic Emission of WSe2 Monolayers by Laser Excitation at Exciton Resonances. *Phys. Rev. Lett.* **2015,** *114* (9), 097403.

(6) Novoselov, K. S.; Jiang, D.; Schedin, F.; Booth, T. J.; Khotkevich, V. V.; Morozov, S. V.; Geim, A. K. Two-dimensional atomic crystals. *Proc. Natl. Acad. Sci. U. S. A.* **2005,** *102* (30), 10451-10453.

(7) (a) He, K. L.; Kumar, N.; Zhao, L.; Wang, Z. F.; Mak, K. F.; Zhao, H.; Shan, J. Tightly Bound Excitons in Monolayer WSe2. *Phys. Rev. Lett.* **2014,** *113* (2), 026803. (b) Chernikov, A.; Berkelbach, T. C.; Hill, H. M.; Rigosi, A.; Li, Y.; Aslan, O. B.; Reichman, D. R.; Hybertsen, M. S.; Heinz, T. F. Exciton Binding Energy and Nonhydrogenic Rydberg Series in Monolayer WS2. *Phys. Rev. Lett.* **2014,** *113* (7), 076802. (c) Dinh Van, T.; Yang, M.; Dery, H. Coulomb interaction in monolayer transition-metal dichalcogenides. *Phys. Rev. B* **2018,** *98* (12), 125308.

(8) (a) Liu, X.; Galfsky, T.; Sun, Z.; Xia, F.; Lin, E.-c.; Lee, Y.-H.; Kena-Cohen, S.; Menon, V. M. Strong light-matter coupling in two-dimensional atomic crystals. *Nature Phot.* **2015,** *9* (1), 30-34. (b) Low, T.; Chaves, A.; Caldwell, J. D.; Kumar, A.; Fang, N. X.; Avouris, P.; Heinz, T. F.; Guinea, F.; Martin-Moreno, L.; Koppens, F. Polaritons in layered two-dimensional materials. *Nat. Mater.* **2017,** *16* (2), 182-194. (c) Schneider, C.; Glazov, M. M.; Korn, T.; Hoefling, S.; Urbaszek, B. Two-dimensional semiconductors in the regime of strong light-matter coupling. *Nat. Commun.* **2018,** *9*, 2695.

(9) (a) Raja, A.; Chaves, A.; Yu, J.; Arefe, G.; Hill, H. M.; Rigosi, A. F.; Berkelbach, T. C.; Nagler, P.; Schueller, C.; Korn, T.; Nuckolls, C.; Hone, J.; Brus, L. E.; Heinz, T. F.; Reichman, D. R.; Chernikov, A. Coulomb engineering of the bandgap and excitons in two-dimensional materials. *Nat. Commun.* **2017,** *8*, 15251. (b) Mao, N.; Chen, Y.; Liu, D.; Zhang, J.; Xie, L. Solvatochromic effect on the photoluminescence of MoS_2 monolayers. *Small*, **2013**, *9*, 1312. (10) Kelly, K. L.; Coronado, E.; Zhao, L. L.; Schatz, G. C. The optical properties of metal nanoparticles: The influence of size, shape, and dielectric environment. *J. Phys. Chem. B* **2003,** *107* (3), 668-677.

(11) Schaller, R. D.; Lee, L. F.; Johnson, J. C.; Haber, L. H.; Saykally, R. J.; Vieceli, J.; Benjamin, I.; Nguyen, T. Q.; Schwartz, B. J. The nature of interchain excitations in conjugated polymers: Spatially-varying interfacial solvatochromism of annealed MEH-PPV films studied by near-field scanning optical microscopy (NSOM). *J. Phys. Chem. B* **2002,** *106* (37), 9496-9506.

(12) (a) Castellanos-Gomez, A.; Roldán, R.; Cappelluti, E.; Buscema, M.; Guinea, F.; van der Zant, H. S. J.; Steele, G. A. Local strain engineering in atomically thin MoS2. *Nano Lett.* **2013,** *13* (11), 5361. (b) Khestanova, E.; Guinea F.; Fumagalli, L.; Geim, A. K.; Grigorieva, I. V. Universal shape and pressure inside bubbles appearing in van der Waals heterostructures. *Nat. Commun.* **2016**, *7*, 12587.

(13) Scully, M. O.; Fleischhauer, M. Lasers without inversion. *Science* **1994,** *263* (5145), 337-338.

(14) Longdell, J. J.; Fraval, E.; Sellars, M. J.; Manson, N. B. Stopped light with storage times greater than one second using electromagnetically induced transparency in a solid. *Phys. Rev. Lett.* **2005,** *95* (6), 063601.

(15) Saffman, M.; Walker, T. G.; Molmer, K. Quantum information with Rydberg atoms. *Rev. Mod. Phys.* **2010,** *82* (3), 2313-2363.

(16) Castellanos-Gomez, A.; Buscema, M.; Molenaar, R.; Singh, V.; Janssen, L.; van der Zant, H. S. J.; Steele, G. A. Deterministic transfer of two-dimensional materials by all-dry viscoelastic stamping. *2D Mater.* **2014,** *1* (1), 011002.

(17) (a) The above-gap conduction-band edges (CB+2) are contributed mostly from the *d*-orbitals of tungsten, i.e. the d_{xy} and $d_{x^2-y^2}$ orbitals. (b) Liu, G.–B.; Xiao, D.; Yao, Y.; Xu, X.; Yao, W. Electronic structures and theoretical modelling of two-dimensional group-VIB transition metal dichalcogenides. *Chem. Sov. Rev.* **2015**, *44*, 2643-2663. (c) Kormányos, A.; Burkard, G.; Gmitra, M., Fabian, J.; Zólyomi, V.; Drummond, N. D.; Fal'ko, V. k·p theory for two-dimensional transition metal dichalcogenide semiconductors. *2D Mater*. **2015**, *2*(2), 022001. (d) Glazov, M. M.; Golub, L. E.; Wang, G.; Marie, X.; Amand, T.; Urbaszek, B. Intrinsic exciton-state mixing and nonlinear optical properties in transition metal dichalcogenide monolayers. *Phys. Rev. B* **2017,** *95* (3), 035311.

(18) Scuri, G.; Zhou, Y.; High, A. A.; Wild, D. S.; Shu, C.; De Greve, K.; Jauregui, L. A.; Taniguchi, T.; Watanabe, K.; Kim, P.; Lukin, M. D.; Park, H. Large Excitonic Reflectivity of Monolayer MoSe2 Encapsulated in Hexagonal Boron Nitride. *Phys. Rev. Lett.* **2018,** *120* (3), 037402.

(19) Beal, A.; Knights, J.; Liang, W. Transmission spectra of some transition metal dichalcogenides. II. Group VIA: trigonal prismatic coordination. *J. Phys. C Sol. Stat.* **1972**, *5*, 3540–3551.

(20) (a) Xu, X.; Yao, W.; Xiao, D.; Heinz, T. F. Spin and pseudospins in layered transition metal dichalcogenides. *Nat. Phys.* **2014**, *10*, 343. (b) Manca, M.; Glazov, M. M.; Robert, C.; Cadiz, F.; Taniguchi, T.; Watanabe, K.; Courtade, E.; Amand, T.; Renucci, P.; Marie, X.; Wang, G.; Urbaszek, B. Enabling valley selective exciton scattering in monolayer WSe2 through upconversion. *Nat. Commun.* **2017,** *8*, 14927.

Table of Contents artwork

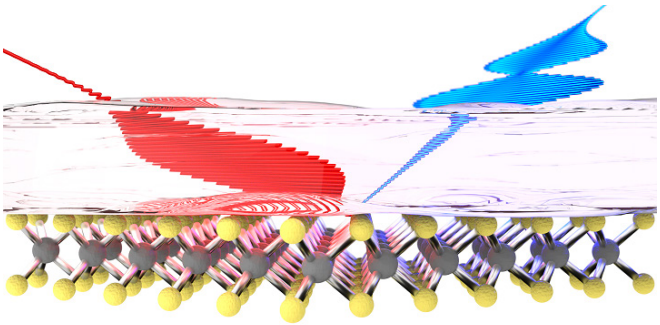

Supporting information

Polymer overlayers tune electromagnetically induced transparency in a two-dimensional semiconductor

Kai-Qiang Lin, Robert Martin, Sebastian Bange, John M. Lupton*

Institut für Experimentelle und Angewandte Physik, Universität Regensburg, Universitätsstraße 31, 93053 Regensburg, Germany

Experimental Section

Sample preparation

Monolayer WSe_2 and few-layer hBN samples were obtained through mechanical exfoliation[1,2] from bulk crystals (HQ graphene). We stamp the monolayer WSe_2 and the hBN through a dry-transfer technique using commercial PDMS films (Gel-Pak, Gel-film X4). To fabricate polymer-covered WSe_2, we stamp the monolayer WSe_2 on Si/SiO_2 wafers first and then spin coat poly(methyl methacrylate) (PMMA; M_w 97,000; Sigma-Aldrich), polystyrene (PS; M_w 290,000; Sigma-Aldrich), the cycloolefin copolymer Zeonex® (330R) (Zeon Corp.), PMMA-PS 1:1 copolymer (PMMA-PS1; M_n 30,000; Sigma-Aldrich), PMMA-PS 1:2 copolymer (PMMA-PS2; M_n 82,000; Sigma-Aldrich), polyethylene (PE; M_w 35,000; Sigma-Aldrich) or poly(acrylic acid) (PAA; M_v 450,000; Sigma-Aldrich). PMMA, PS, PMMA-PS copolymers, Zeonex, and PE were dissolved toluene at a weight/weight concentration of 2 %. PAA was dissolved in ethanol weight/weight concentration of 2 %. Spin coating was performed at a speed of 2000 rounds/min for the duration of 1 min.

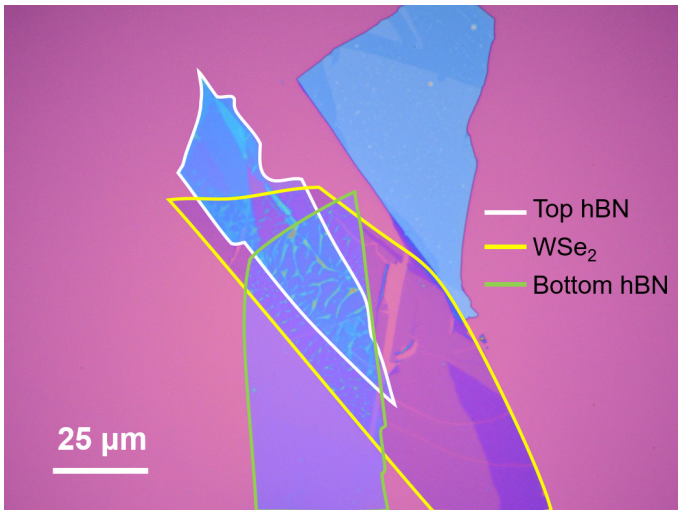

Figure S1. Microscope image of the monolayer WSe_2 sample encapsulated by two multilayers of hBN on a silicon wafer with a 300 nm thermal oxide layer on top.

Optical measurements

The setup and experimental information were detailed in Ref 1. Briefly, we cool down the sample to 5 K in a helium microscope cryostat (Janis, ST-500). With a 0.6 NA objective (Olympus, LUCPLFLN 40X) we observe the sample and focus the laser onto the sample. We first measured the photoluminescence of the monolayer WSe_2 under 488 nm excitation (argon-ion laser, Spectra Physics, 2045E). A 488 nm long-pass edge filter (Semrock, LP02-488RU) was used to filter out the laser line. To measure the electromagnetically induced transparency in second-harmonic generation (SHG), we used a 80 fs pulsed Ti:sapphire laser (Spectra-Physics, Mai Tai XF). A 680 nm short-pass edge filter (Semrock, FF01-680SP) was used to filter out the excitation pulse to record the SHG signal.

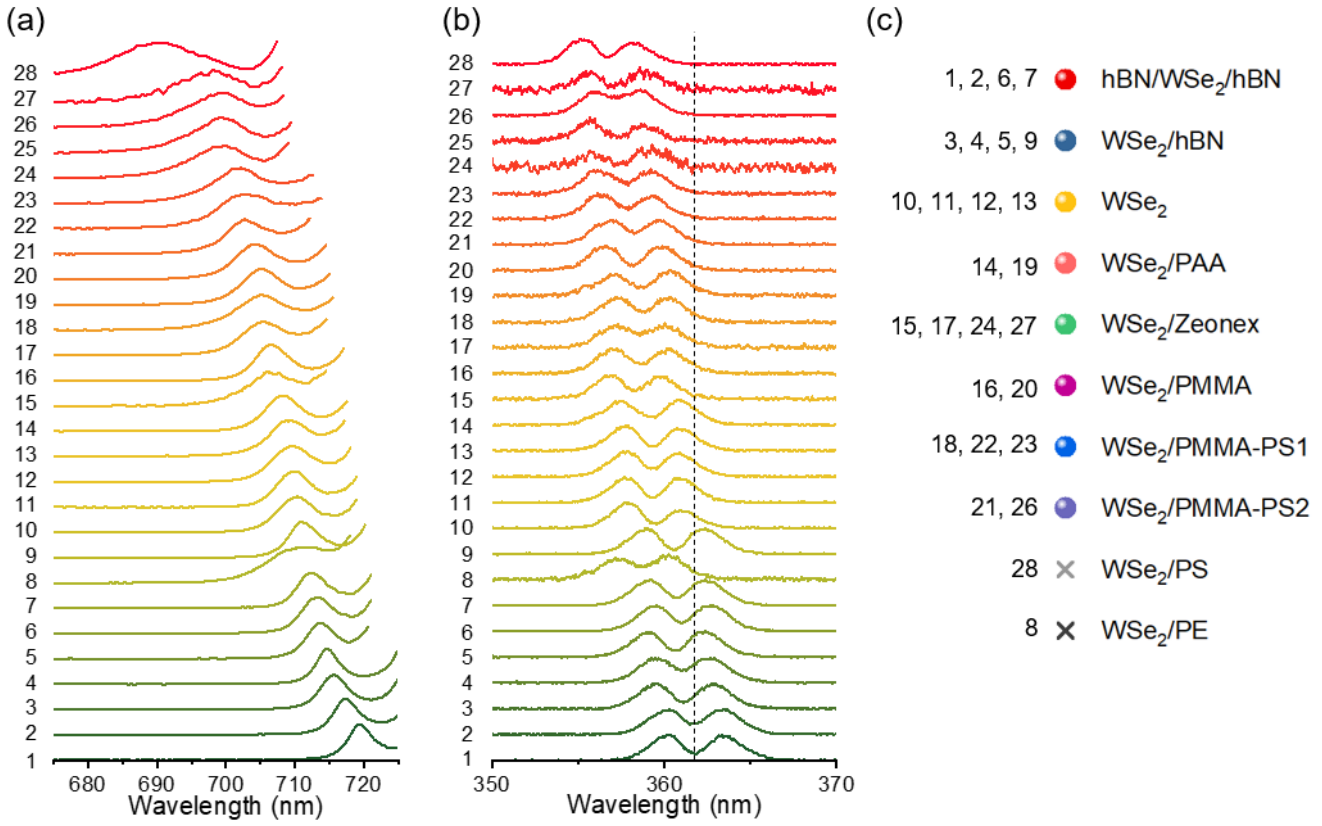

Figure S2. Plots of PL (a) and SHG (b) spectra of all WSe_2 samples studied, ordered by PL peak energy. Panel (c) shows the corresponding labeling. The PS (No. 28) and PE (No. 8) covered samples show anomalously broad PL spectra and do not follow the linear correlation in Fig. 3 of the main text.

References

(1) Lin, K.-Q.; Bange, S.; Lupton, J. M. *Nat. Phys.* **2019**, *15*, 242-246.

(2) Castellanos-Gomez, A.; Buscema, M.; Molenaar, R.; Singh, V.; Janssen, L.; van der Zant, H. S. J.; Steele, G. A. *2D Mater.* **2014,** *1* (1), 011002.